Artículo invitado: Revisión de la técnica de multiplexación por divisiones de frecuencias ortogonales (OFDM)

A. J. Zozaya

Laboratorio de Electromagnetismo Aplicado (LaBEMA), Facultad de Ingeniería, Universidad de Carabobo

Resumen.-

La técnica de Multiplexación por División de Frecuencias Ortogonales (OFDM) es el esquema de modulación más ampliamente usado en los sistemas de comunicaciones modernos. En este artículo se describen los principios básicos de funcionamiento de ésta técnica mediante la simulación de un sistema OFDM simplificado.

Palabras clave: Multiplexación por División de Frecuencias Ortogonales (OFDM), Modulación de Amplitud en Cuadratura M-aria (M-QAM), Alinealidades de los AP de banda estrecha.

Paper invited: Orthogonal Frequency Division Multiplexing revisited (OFDM)

Abstract.-

Orthogonal Frequency Division Multiplexing (OFDM) is the modulation scheme most widely used in modern telecommunication systems. In this article the basics of such technique are described. A simplified simulation model of an OFDM system is used for this purpose.

Keywords: Orthogonal Frequency Division Multiplexing (OFDM), M-ary Quadrature Amplitude Modulation (M-QAM), Narrowband PA nonlinearities.

1. Introduction

Orthogonal Frequency Division Multiplexing (OFDM) is a modulation scheme widely used in modern telecommunication systems. Among today telecommunication systems we find the very popular DSL for wired communication, Wi-Fi for local wireless communication, and LTE for mobile communication. All them use OFDM as their standard modulation technique. ODFM combines the M-ary quadrature amplitude modulation (M-QAM) scheme with orthogonal frequency modulation technique. The main advantage of OFDM technique resides in its capability of accommodate more bits per bandwidth than any other modulation technique. In this article the basics of the Orthogonal Frequency Division Multiplexing technique are presented. The article is organized as follow. In Section 2 the general architecture of an OFDM system is presented. In Section 3 a baseband model is described. The baseband model is then used as a benchmark for the rest of the article. However, references to the RF model are made throughout the paper when it is necessary to give a more precise description of concepts. In order to illustrate the main principles of Orthogonal Frequency Division Multiplexing technique a very simple simulation of an OFDM system is discussed in Section 4. In Section 4 a time evolution of signals of interest from digital domain to analog domain is included. The nonlinearity issue of power amplification by using a narrowband nonlinearities model for the Power Amplifier (PA) is also discussed in Section 4. A short conclusion is given in Section 5.

Correo-e: `azozaya@uc.edu.ve` (A. J. Zozaya)

2. General architecture of an OFDM system

Simplified models of OFDM transmitter and OFDM receiver systems are given in Figure 1.

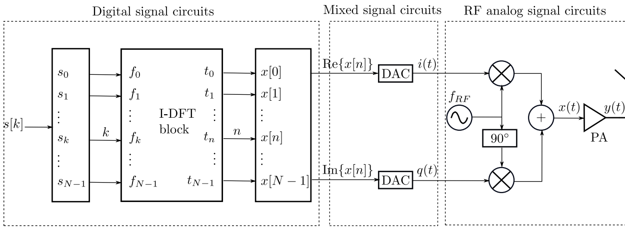

(a) OFDM transmitter

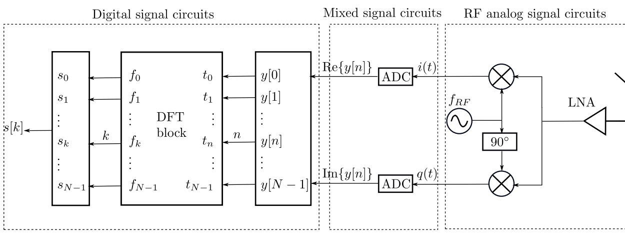

(b) OFDM receiver

Figura 1: Simplified models of OFDM Tx and Rx systems.

As it is shown in Fig. 1 an OFDM system has a baseband (or digital) module, an RF analog circuitry, and an hybrid (or mixed signal) module in between. The signal $x(t)$ in the Fig. 1 is the input signal to the power amplifier (PA) and it has the form:

$$x(t) = a(t)\cos[\omega_{RF}t + \varphi(t)] \tag{1}$$

where $[a(t), \varphi(t)]$ corresponds to an OFDM symbol during a time equal to the OFDM symbol duration. A complex OFDM symbol $s_{OFDM}(t)$ admits (obsviously) a polar form $s_{OFDM}(t) = a(t)\mathrm{e}^{\jmath\varphi(t)}$ called complex amplitude of $x(t)$, or an equivalente cartesian representation $s_{OFDM}(t) = i(t) + \jmath q(t)$, where $i(t)$ is the in-phase component and $q(t)$ is the quadrature component of the complex amplitude. The output $y(t)$ of the power amplifier (PA), in the main harmonic zone, has the form:

$$y(t) = A(a)\cos[\omega_{RF}t + \varphi(t) + \Phi(a)]$$

where $A = A(a)$ and $\Phi = \Phi(a)$ are the so called AM/AM and AM/PM conversion functions of the PA, respectively. Such functions model the narrowband nonlinearities of the PA at baseband frequencies. The impact of the AM/AM and AM/PM conversion functions of the PA in the system performance will be discussed briefly later.

3. Baseband model of an OFDM system

For didactic and simulation purposes the Tx-Rx model shown in Fig. 1 has been replaced by the baseband (or complex) model shown in Fig. 2.

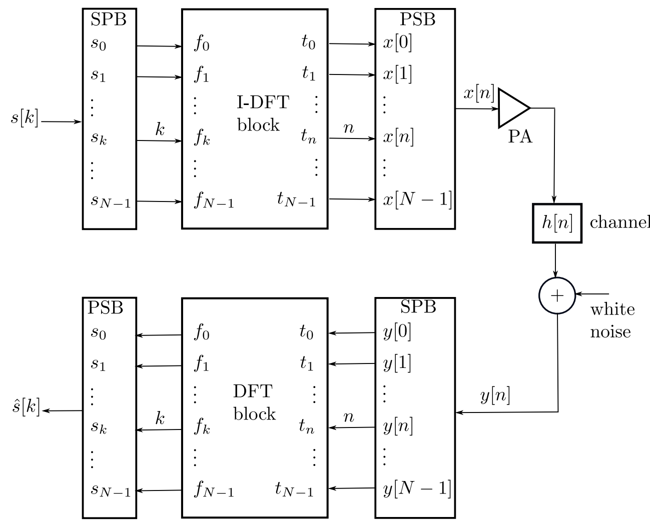

Figura 2: Baseband model of a TxRx OFDM system.

In Figure 2 the RF and mixed signal circuits have been suppressed and the digital part plus the complex model of the PA have been retained. In this model $s[k]$ is the k^{th} input symbol at discrete time k to the series to parallel block (SPB). Input symbols are generated at a rate of $1/T_s$ symbols per second. The series to parallel block (SPB) converts a series stream of N symbols in an array $[s_{0,} s_{1,}, \ldots, s_k, \ldots, s_{N-1}]$ of N symbols which are passed in parallel to the I-DFT block at a rate of $1/NT_s$ packets of symbols per second. The I-DFT block composes an OFDM symbol by adding N weighted harmonically related complex exponentials in the form:

$$x[n] = \frac{1}{N}\sum_{k=0}^{N-1} s[k]\mathrm{e}^{\frac{\jmath 2\pi kn}{N}} \qquad n = 0, 1 \ldots n \ldots N-1 \tag{2}$$

where $x[n]$ is the n^{th} sample of the OFDM baseband discrete signal at the output of the I-DFT block. These complex exponentials $\exp(\jmath 2\pi \mathrm{k/N})$

are harmonically related because of they oscillate at discrete frequencies which are all multiples of $\Delta f = 1/N$, hence they are orthogonal. The output array of the I-DFT block is converted to a series stream of time discrete samples in the parallel to series block (PSB). Samples $x[n]$ feed the power amplifier. The PA output is convolved with the impulsive transfer function $h(n)$ of the channel. The impulsive response of the channel depends on the application, but usually it models some kind of multipah fading. Gaussian white noise is added to take account for general thermal noise. The power of noise added is calibrated from the formula $P_n = -174\text{dBm} + 10\log(\text{BW})$, where BW is the bandwith of the system. Signal $y[n]$ is the n^{th} sample of the OFDM discrete signal at the input of the receiver after amplfication, transmision through the channel and adding some amount of white noise. A process which is the converse of the transmitter takes place at the reciever. Series samples $y[n]$ are passed in parallel to the DFT block by the SPB. The DFT block takes the N samples of $y[n]$ for extracting from them their spectrum $[s_{0,} s_{1,} \ldots, s_k, \ldots, s_{N-1}]$:

$$\hat{s}[k] = \sum_{n=0}^{N-1} x[n] e^{-\frac{j2\pi kn}{N}} \qquad k = 0, 1 \ldots n \ldots N-1$$

This spectrum $[s_k]$ contains the estimated symbols $\hat{s}[k]$.

All previous signals are discretes and complexes (obviously), and (in general) their real parts correspond to the in-phase components whilst their imaginary parts correspond to the quadrature components of the real baseband signals. The model presented in Fig. 2 will be used as a framework through the rest of this article.

4. Some simulation results

The system of Fig. 2 was tested using a family of QPSK symbols onto 16 subcarriers. A sequence of 20480 bits was generated randomly to feed a bit to QPSK symbol mapper block (no included in either both figures 1 and 2). These bits are mapped onto QPSK symbols in accordance with the assignment law that is shown in Table (1).

Table 1: Assignment law used in mapping bits onto QPSK symbols.

bits	logical value of the QPSK symbol	numerical value of the QPSK symbol
00	0	$\exp(\jmath\pi/4)$
01	1	$\exp(\jmath 3\pi/4)$
10	2	$\exp(-\jmath\pi/4)$
11	3	$\exp(-\jmath 3\pi/4)$

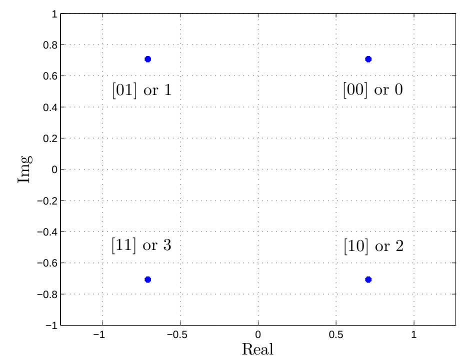

Figura 3: QPSK symbols constellation.

The mapping process in accordance with the assignment law presented in Table 1 is carried out in the digital signal circuits via software. The QPSK symbol time duration was set to $T_s = 2$ [sec].

In Fig. (3) the location of QPSK symbols in the complex plane is presented. It is is called the QPSK symbols constellation.

The stream of QPSK symbols obtained from the bits to symbol mapper are packet in parallel arrays in the PSB (forming the corresponding OFDM symbols in the frequency-domain) to feed the I-DFT block. The resulting OFDM symbols have a time duration of $T_{OFDM} = 32$ [sec], and such symbols convey 16 QPSK symbols each. Subcarriers generated at the I-DFT block are separated $\Delta f = 1/32$ Hz from each other, and together they span a bandwidth of BW=0.5 Hz . The spectrum of $x[n]$ is presented in Fig. 4. From the I-DFT process a stream of parallel packets containing $N = 32$ time samples of the OFDM symbol results. A cyclic prefix of 8 [sec] (that is 4 samples more) is added. As cyclic prefix the last eight samples of each OFDM symbol are replicated at the beginning of it in the form: $\{x[n]\} = \{[x[13:16]\ x[1:16]\}$. These parallel frames are then converted to a series stream of samples $x[n]$ in the time-domain. Now, each OFDM symbol has a time duration of 40 [sec].

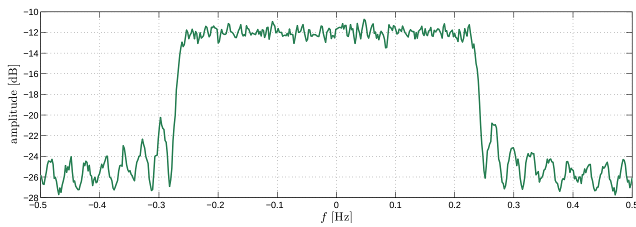

Figura 4: Spectrum of $x[n]$

4.1. *Time domain considerations*

In this Section we will take a look at the time-domain evolution of signals of interest, departing from the baseband discrete and continous time signals and finishing in the RF continous time signal. The digital signal $x[n]$ is split inside the digital circuitry in its real Real$\{x[n]\}$ and imaginary Img{x[n]} components. The in-phase $i(t)$ and quadrature $q(t)$ continous signals (see Fig. (1)) are obtained from the sequences Real$\{x[n]\}$ and Img{x[n]} by interpolation and filtering. Interpolation allows to fill the empty spaces between samples and the filtering process eliminates the high frequency content resulting from a zero order interpolation. In Figs. 5 through 7 the evolution of the sequence Img{x[n]} (in discrete time), to signal $q(t)$ (in continous time) for one given OFDM symbol period is presented in order to ilustrate their relationship.

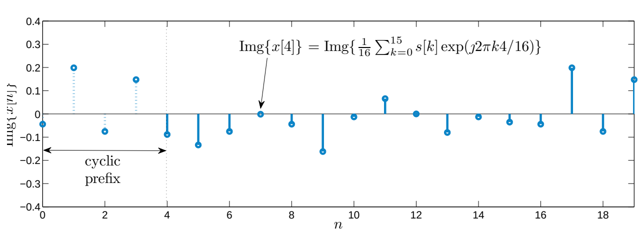

Figura 5: Time-domain evolution of an OFDM symbol from digital to analog domain. Detail of the discrete-time sequence Img$\{x[n]\}$

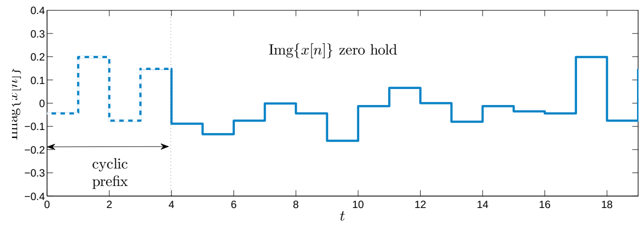

Figura 6: Time-domain evolution of an OFDM symbol from digital to analog domain. Detail of the discrete-time sequence Img$\{x[n]\}$ after zero hold interpolation.

In Fig. 5 some samples of the imaginary parts of $x[n]$ (for one OFDM symbol) inside the digital circuitry are shown. The sequence $x[n]$ is zero order hold interpolated inside the mixed signal circuits of Fig. 1. In Fig. 6 the resulting stairs shaped continous time signal is plotted.

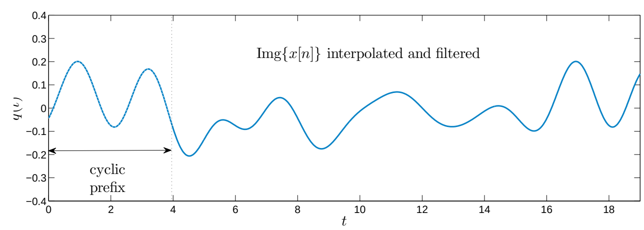

Figura 7: Time-domain evolution of an OFDM symbol from digital to analog domain. Detail of continous-time signal $q(t)$.

Signal $q(t)$ is obtained from the previous zero hold retained signal by means of filtering. The filtering process eliminate the high frequency content of the interpolated signal. The resulting signal $q(t)$ is shown in Fig. 7. Exactly the same process apply to $i(t)$ regarding Re$\{x[n]\}$. Signals $i(t)$ and $q(t)$ are analog baseband signals, and their bandwidth is 0.5 Hz. Both these signals feed the IQ modulator inside the RF analog circuits of Fig. 1. The IQ modulator constructs the signal $x(t)$ given in Eq. (1).

The amplitude $a(t)$ of the RF signal $x(t)$ at the PA input is composed by signals $i(t)$ and $q(t)$ in the form $a(t) = \sqrt{i^2(t) + q^2(t)}$. The elongation of $a(t)$ is of primary concern to the PA designer. In Figure 8 the corresponding amplitude $a(t)$ of the resulting OFDM RF signal at the PA input is shown. The resulting RF signal has an RMS value of 0.1249 [V] and a peak value of 0.3795

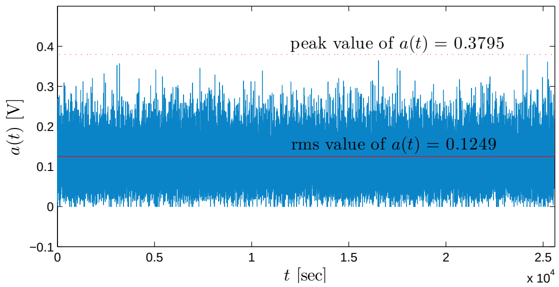

Figura 8: Amplitude $a(t)$ of the ODFM RF signal $x(t) = a(t)\cos[\omega_{RF}t + \varphi(t)]$ at the input of the PA resulting from the modulation of 16 subcarriers with a QPSK scheme. This picture corresponds to 640 OFDM symbols (or 10240 QPSK symbols, or 20480 bits).

[V], and consequently a crest factor C, given as $C = x_{peak}/x_{RMS}$, of $C = 3{,}038$. The peak-to-average power ratio (PAPR) of $x(t)$ is PAPR(dB) = $20\log C = 9{,}652$dB.

Making a zoom of Fig. 8 $a(t)$ could be observed in more detail. In Fig. 9 the amplitude $a(t)$ for three consecutive OFDM symbols is shown.

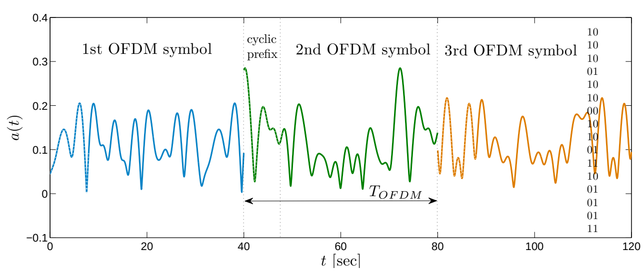

Figura 9: Amplitude $a(t)$ of the ODFM RF signal for three consecutive OFDM symbols. .

By folding the plot in Fig. 9 around the time axis, the reader (who is no confortable with baseband models and signals) can imagine the RF carrier oscillating rapidly (at RF) within $a(t)$ and $-a(t)$ with a time varying phase $\varphi(t)$. The quantities $a(t)$ and $\varphi(t)$ contain half the information each, whilst the carrier does transport them along the channel.

4.2. *PA Nonlinearity considerations*

In order to investigate the impact of the PA nonlinearities in the OFDM signal a simple simulation was carried out. Here we will concern only on short–term nonlinearities [1]. For such

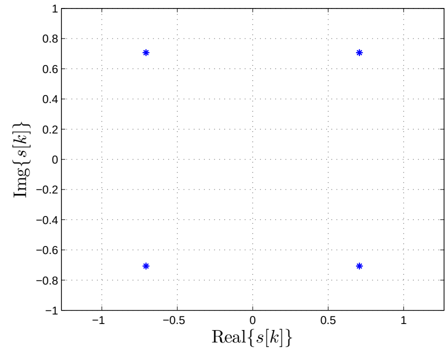

(a) Scatter plot of transmitted symbols

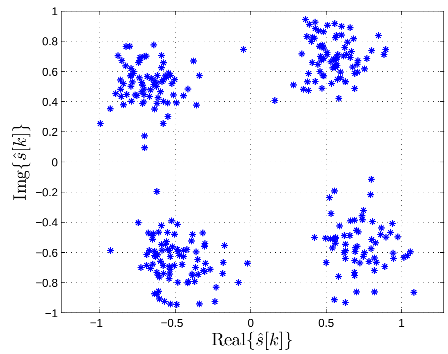

(b) Scatter plot of estimated symbols at the reciever

Figura 10: Scatter plots.

purpose the AM/AM and AM/PM conversion functions are sufficient enough to model the PA [2]. The former function was modeled using a cubic polynomial, and their parameters were set in order to have a third-order interception point (IP_3 or TOI) at 25 dBm of input power. Recall that from a simplified analysis, the 1 dB compression point occurs approximately 9.6 dB below the third-order intercept point. The AM/PM function was also incorporated by setting 10 degrees of rotation per dB from a minimum of 15 dBm of power input. White noise with a power of σ^2(dBm) $= -3$dBm was added to $x[n]$ to obtain $y[n]$. In the Figure 10 the scatter diagrams of transmitted symbols –Fig. 10(a)– and estimated symbols at the receiver –Fig. 10(b)– are shown.

From Figure 10 it can be observed that the AM/AM conversion function compresses the symbol's constellation whilst the AM/PM conversion function rotates it. In our simulation, the rate of degrees of rotation per input power (beyond

15 dBm) was exaggerated for didactic purposes. Dispersion of symbols in Fig. 10(b) are due to white noise. The noise added in our simulation was also inflated for didactical purpose. Dispersion due to white noise in conjunction with the AP compression and rotation cause signal distortion. Signal distortion yields out-band spectral regrowth and increasing bit errors. In more realistic communication systems (the modern ones), the OFDM carriers are usually modulated with constellations which are denser than the QPSK diagram. Indeed a M–QAM scheme is used, where M could be 16, 32, 64, or greater yet. Recall that $M = 2^N$, where N in the number of bits maped on a M–OAM symbol. The grater number M the higher distortion due to PA nonlinearities. For alleviating the distortion caused by the PA nonlinearities some linearization technic must be used and so an extra hardware together with some extra software must be incorporated to the transmitter. Linearization of Power Amplifiers is a vast area of research and it is out of the scope of this article. Readers interested in PA linearization techniques are encouraged to read Refs [3].

5. Conclusion

In this article a tutorial description of a OFDM system was presented. Details on time evolution of signals of interest were also given, and finally, the nonlinearities issue due to power amplification was discussed briefly.

Referencias

[1] Lei Ding. Digital Predistortion of Power Amplifiers for Wireless Applications. PhD thesis, School of Electrical and Computer Engineering, Georgia Institute of Technology, 2004.

[2] Raviv Raich and G. Tong Zhou. On the modeling of memory nonlinear efects of power amplifiers for communication applications. Digital Signal Processing Workshop, 2002 and the 2nd Signal Processing Education Workshop. Proceedings of 2002 IEEE 10th, pages 7–10, 2002.

[3] Steve C. Cripps. RF Power Amplifiers for Wireless Communications. Artech House, 2006.

[4] Earl McCune. Microwave bytes: This emperor has no clothes? IEEE Microwave Magazine, pages 48–2, 2013.

[5] Ashwin Prasad. Gaining spectral efficiency with ofdm. Microwave Journal, pages 1–, 2007.

Alfonso J. Zozaya received the electronic engineering degree from the Polytechnic University of the National Armed Forces (IUPFAN), Maracay, Venezuela, in 1991 and the Doctor degree from the Polytechnic University of Catalonia (UPC), Barcelona, Spain, in 2002. He is Full Professor at the Telecommunication School of the University of Carabobo, Valencia, Venezuela. He is the founder of the Applied Electromagnetics Laboratory (LaBEMA) of the University of Carabobo. His research interests are in the areas of applied electromagnetics, computational electromagnetics, and RF power amplifier linearization techniques.